Vol. **113** (2008) *ACTA PHYSICA POLONICA A* No. 6

Synthesis by Wet Chemical Method and Characterization of Nanocrystalline ZnO Doped with Fe_2O_3

U. Narkiewicz[a], D. Sibera[a], I. Kuryliszyn-Kudelska[b], L. Kilański[b], W. Dobrowolski[b] and N. Romčević[c]

[a]Szczecin University of Technology
Institute of Chemical and Environment Engineering
Pułaskiego 10, 70-322 Szczecin, Poland
[b]Institute of Physics, Polish Academy of Sciences
al. Lotników 32/46, 02-668 Warszawa, Poland
[c]Center for Solid State Physics and New Materials, Institute of Physics
Pregrevica 118, 11080 Belgrade, Serbia

(Received February 8, 2008)

Nanocrystalline samples of ZnO doped with Fe_2O_3 were synthetized by wet chemical method. The series of ZnO nanosized samples in the wide range of Fe_2O_3 concentration (from 5 wt.% to 95 wt.%) was prepared by precipitation from nitrate solutions using ammonia. The phase composition of the samples was determined using X-ray diffraction measurements. The phases of hexagonal ZnO, and/or rhombohedric Fe_2O_3, and/or $ZnFe_2O_4$ were identified. The mean crystalline size of nanocrystals, determined with the use of Scherrer's formula, varied from 8 to 52 nm. The preliminary micro-Raman spectroscopy measurements were performed. The observed features are typical of Fe doped ZnO nanoparticles. The magnetic measurements revealed the presence of different types of magnetic behavior. For samples with high Fe_2O_3 contents (above 70 wt.%) the ferromagnetic ordering was observed at room temperature. For samples with lower Fe_2O_3 contents we observed the phenomenon of superparamagnetism above the blocking temperature.

PACS numbers: 81.07.–b, 75.75.+a, 78.67.Bf

1. Introduction

Recently, a continued interest in the synthesis and properties of nanoscale inorganic materials has been observed. Semiconductor nanocrystals have been of much interest over two decades because of their unique physical properties result-

ing from the modification of the electronic states due to the confinement effect. Currently, nanostructures made of ZnO have attracted significant attention owing to their proposed applications in low-voltage and short-wavelength electro-optical devices, transparent ultraviolet protection films, and spintronic devices [1, 2].

A considerable attention has recently been devoted to high temperature ferromagnetism observed in transition-metal doped oxides. Particularly ZnO has been identified as a promising host semiconductor material, exhibiting ferromagnetism when doped with most of the transition metal elements — V, Cr, Fe, Co, Ni [3]. However, the origin of ferromagnetic behavior is not very well known in these compounds. Recently, it was shown that the ferromagnetism in these materials can be induced by inclusions of nanoscale oxides of transition metals [4] and/or nanoparticles containing a large concentration of magnetic ions [5]. Novel methods enabling a control of nanoassembling of magnetic nanocrystals in nonconducting matrices as well as functionalities specific to such systems were described [5].

The aim of this work was to synthetize the series of nanosized ZnO powders doped with iron oxide. The samples were characterized by means of X-ray diffraction and scanning electron microscopy. The preliminary micro-Raman investigations were performed. The preliminary magnetic studies were carried out.

2. Experimental

The samples were synthetized with the use of wet chemical method. First, the mixture of iron and zinc hydroxides was obtained by addition of an ammonia solution to the 20% solution of proper amount of $Zn(NO_3) \cdot 6H_2O$ and $Fe(NO_3)_3 \cdot 4H_2O$ in water. Next, the obtained hydroxides were filtered, dried and calcined at 300°C during 1 h. A series of samples containing from 5 to 95 wt.% of Fe_2O_3 was obtained.

The phase composition of the samples was determined with the use of X-ray diffraction (Co K_α radiation, X'Pert Philips). The crystalline phases of hexagonal ZnO, and/or rhombohedric Fe_2O_3, and/or cubic $ZnFe_2O_4$ were identified. The typical spectra are shown in Fig. 1. XRD data allowed to determine a mean crystallite size in prepared samples with the use of Scherrer's formula [6]. The mean crystallite size of these phases varied from 8 nm to 52 nm.

The results of XRD measurements, i.e. the phase compositions as well as mean crystallite size are gathered in Table.

The morphology of the samples was investigated using scanning electron microscopy (see Fig. 2). The spherical and elongated nanograins were observed. The degree of agglomeration depended on the amount of Fe_2O_3 and it was smallest in the sample containing 80 wt.% of Fe_2O_3 (DS80Fe20Zn) and greatest in the sample containing 20 wt.% of Fe_2O_3 ($(ZnO)_{0.80}(Fe_2O_3)_{0.20}$). In the sample containing 50 wt.% of Fe_2O_3 (DS50Fe50Zn), the elipsometric forms of agglomerates can be distinguished.

The micro-Raman spectra were taken in the backscattering configuration and analyzed using a Jobin Yvon T64000 spectrometer, equipped with nitrogen cooled

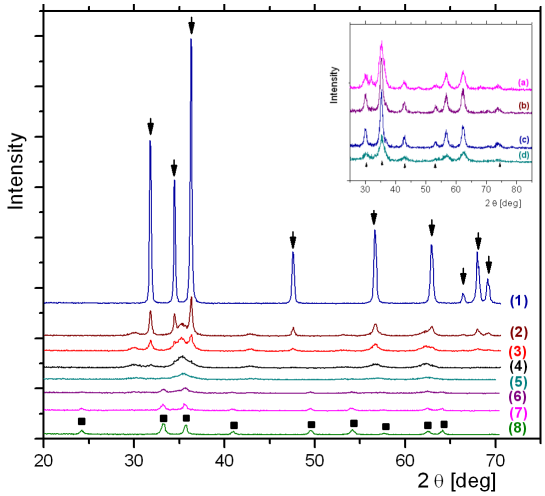

Fig. 1. The results of X-ray diffraction measurements. The selected spectra for several nanocrystalline samples of ZnO doped with Fe_2O_3 are shown: line (1) corresponds to ZnO sample; (2) — DS30Fe70Zn; (3) — DS40Fe60Zn; (4) — DS50Fe50Zn; (5) — DS80Fe20Zn; (6) — DS90FeZn10; (7) — DS95Fe5Zn; (8) — Fe_2O_3. The characteristic peaks attributed to ZnO (arrows) and Fe_2O_3 (squares) are marked. The inset shows the five characteristic peaks attributed to $ZnFe_2O_4$ for selected samples: line (*a*) corresponds to DS50Fe50Zn sample; (*b*) — DS60Fe40Zn sample; (*c*) — DS70Fe30Zn; (d) — DS80FeZn20. It is clearly visible that phases of hexagonal ZnO, and/or rhombohedric Fe_2O_3, and/or cubic $ZnFe_2O_4$ can be distinguished in the synthetized nanocrystals.

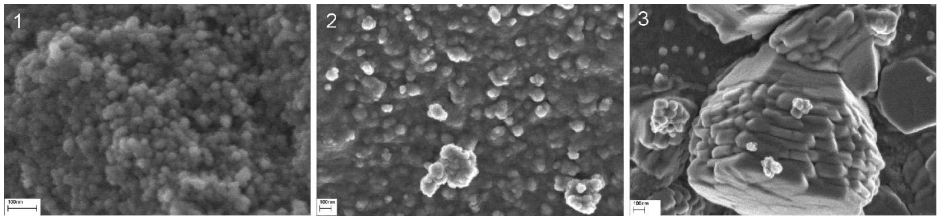

Fig. 2. SEM image for three samples of nanosized ZnO doped with Fe_2O_3. Part 1 corresponds to sample DS80Fe20Zn (80 wt.% of Fe_2O_3), part 2 — DS50FeZn50 (50 wt.% of Fe_2O_3), part 3 — $(ZnO)_{80}(Fe_2O_3)_{20}$ (20 wt.% of Fe_2O_3).

charge-coupled-device detector. As an excitation source we used the 514.5 nm line of an Ar-ion laser. The measurements were performed at low laser power (3 mW). Figure 3 shows the Raman spectra of nanocrystalline ZnO sample doped with 5 wt.% of Fe_2O_3 ($(ZnO)_{0.95}(Fe_2O_3)_{0.05}$) obtained at room temperature. A Raman peak at 436 cm^{-1} is clearly visible. This peak is typical of ZnO nanoparticles undoped with transition metals [7]. It should be stressed here that XRD measurements did not reveal the presence of hexagonal ZnO phase in this sample.

TABLE

The results of X-ray diffraction measurements. The identified crystalline phases as well as mean crystallite size $\tilde{a}$ determined with the use of Scherrer's formula are gathered.

Sample number	wt.% of Fe_2O_3 (nominal concentration)	$\tilde{a}$ [nm] ZnO phase	$\tilde{a}$ [nm] $ZnFe_2O_4$ phase	$\tilde{a}$ [nm] Fe_2O_3 phase
$(ZnO)_{0.95}(Fe_2O_3)_{0.05}$	5	–	10	–
$(ZnO)_{0.90}(Fe_2O_3)_{0.10}$	10	–	8	–
$(ZnO)_{0.80}(Fe_2O_3)_{0.20}$	20	–	8	–
DS30Fe70Zn	30	51	11	–
DS40Fe60Zn	40	26	12	–
DS50Fe50Zn	50	–	8	–
DS60Fe40Zn	60	–	12	–
DS70Fe30Zn	70	–	12	–
DS80Fe20Zn	80	–	12	–
DS90Fe10Zn	90	–	–	24
DS95Fe5Zn	95	–	–	23

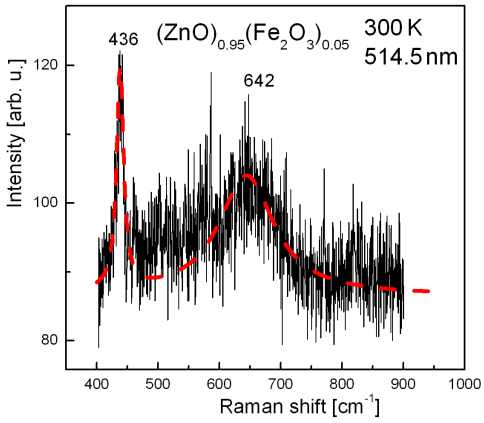

Fig. 3. The room temperature Raman spectra for $(ZnO)_{95}(F_2O_3)_5$ sample (5 wt.% of Fe_2O_3). The solid line corresponds to experiment, the dashed line was added as a guide for eye. A Raman peak at 436 cm^{-1}, typical of undoped ZnO nanoparticles, is clearly observed. A band at 642 cm^{-1}, typical of Fe doped ZnO nanoparticles is pronounced.

Moreover, the Raman spectrum shows also a band at ≈ 642 cm^{-1}. The presence of this band is typical of Fe doped ZnO nanoparticles [7].

The magnetic measurements were performed. The AC magnetic susceptibility χ was measured with the use of mutual inductance method. The real, $\mathrm{Re}(\chi)$, as well as imaginary, $\mathrm{Im}(\chi)$, parts of magnetic susceptibility were determined as a

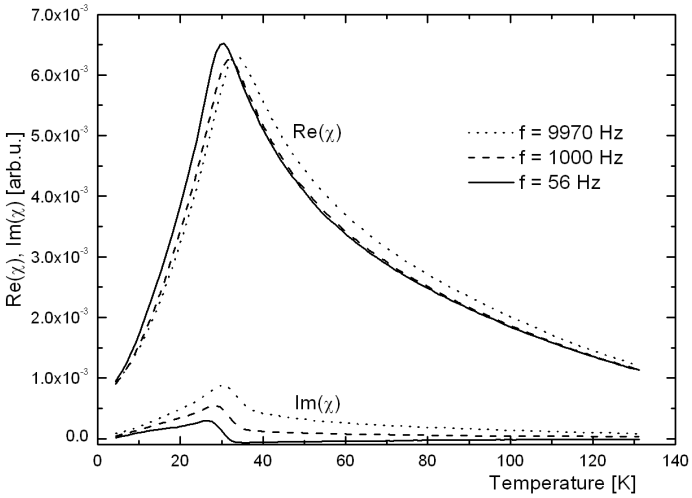

Fig. 4. The temperature dependence of real and imaginary parts of magnetic susceptibility measured for different frequencies (56 Hz, 1000 Hz, 9970 Hz) for ZnO sample with 10 wt% content of Fe_2O_3. The shift of the cusp towards higher temperatures with the frequency increase is clearly visible.

function of temperature and frequency. The temperature dependence of χ at small alternating magnetic field ($H_{\mathrm{AC}} = 5$ Oe and $f = 625$ Hz) in the range between 4.2 K and 300 K was measured. The magnetic measurements were obtained for samples in the wide range of content of Fe_2O_3. We observed different types of magnetic behavior. For samples with high Fe_2O_3 content (70–90 wt.%) the room temperature ferromagnetic ordering is observed. For samples with lower Fe_2O_3 content the characteristic cusp in the real and imaginary part of susceptibility is pronounced. Figure 4 shows the temperature dependence of both parts of magnetic susceptibility measured for different frequencies (56 Hz, 1000 Hz, 9970 Hz) for ZnO sample with 10 wt% content of Fe_2O_3. The shift of this cusp towards higher temperatures with the frequency increase is clearly visible. Such behavior is typical of the phenomenon of the superparamagnetism with the blocking temperature depending on the content of magnetic dopant.

3. Conclusions

ZnO nanopowders doped with iron oxide were obtained by the precipitation method. XRD measurement revealed the presence of three crystalline phases: ZnO, $ZnFe_2O_4$, and Fe_2O_3. The micro-Raman measurements revealed the presence of features typical of ZnO doped with Fe nanoparticles. Different types of magnetic behavior were observed. The samples with high content of Fe_2O_3 are ferromagnetic at room temperature. For samples with low content of Fe_2O_3 we observe behavior typical of superparamagnetism with the blocking temperature shifted in the range 20–40 K.

References

[1] Y. Chen, D.M. Bagnall, H. Koh, K. Park, K. Hiraga, Z. Zhu, T. Yao, *J. Appl. Phys.* **84**, 3912 (1998).

[2] J. Nemeth, G. Rodriguez-Gattorno, A. Vazquez-Olmos, D. Diaz, I. Dekany, *Langmuir* **20**, 2855 (2004).

[3] J.M.D. Coey, M. Venkatesan, C.B. Fitzgerald, *Nat. Mater.* **4**, 173 (2005).

[4] C. Sudakar, J.S. Thakur, G. Lawes, R. Naik, V.M. Naik, *Phys. Rev. B* **75**, 054423 (2007).

[5] T. Dietl, *Acta Phys. Pol. A* **111**, 27 (2007).

[6] A.L. Patterson, *Phys. Rev.* **56**, 978 (1939).

[7] R.Y. Sato-Berru, A. Vázquez-Olmos, A.L. Fernández-Osorio, S. Sortes-Martinez, *J. Raman Spectrosc.* **38**, 1073 (2007).